e-ISSN: 2687-6698 **Research Article**

Turkish Journal of Analytical Chemistry
www.turkjac.org
2019
TurkJAC

Evaluation of photocytotoxic activity of water-soluble Zn(II) phthalocyanine on cancer cells and molecular docking studies

Ugur UZUNER[1], Selcen CELIK-UZUNER[1], Hakkı İsmail KAYA[1,2], Cagla AKKOL[3], Meryem YILMAZ[1], Ece Tugba SAKA[3]*

[1] Karadeniz Technical University, Department of Molecular Biology and Genetics, Trabzon, 61080, Türkiye
[2] Karadeniz Technical University, Department of Biotechnology, Trabzon, 61080, Türkiye
[3] Karadeniz Technical University, Department of Chemistry, Trabzon, 61080, TÜRKİYE

Abstract

In this work, 2(3), 9(10), 16(17), 23(24)-tetrakis-[N-methyl-(1-benzylpiperidin-4-yl)oxy) phthalocyaninato]zinc(II) iodide was synthesized and its aggregation behavior was investigated in different solvents and at varying concentrations. After the cytotoxic effect of 2(3), 9(10), 16(17),23(24)-tetrakis-[N-methyl-(1-benzylpiperidin-4-yl)oxy)phthalocyaninato]zinc(II) iodide was tested, the treatment at certain conditions with phthalocyanine resulted in significant cell death (around 30%) in AR42J pancreatic cancer cells and Sol8 normal muscle cells but the same results were not observed in MDA-MD-231 metastatic breast cancer cells. To evaluate mitochondrial membrane potential (MMP), Mitotracker Red staining was performed and the treatment at certain conditions with 2(3), 9(10), 16(17), 23(24)-tetrakis-[N-methyl-(1-benzylpiperidin-4-yl)oxy)phthalocyaninato]zinc(II) iodide resulted in a significant decrease in mitochondrial membrane potential (represented by $\Delta\psi m$) in MDA-MB-231 cells, but the same situation was not observed in other cells. *In silico* analyses were performed for intracellular target prediction of 2(3), 9(10), 16(17), 23(24)-tetrakis-[N-methyl-(1-benzylpiperidin-4-yl)oxy)phthalocyaninato]zinc(II) iodide and we found that it has inhibitory effects on Sigmar1 protein and Adiponectin receptors 1-2 with the lowest binding energies of (-13.07kcal/mol, -10.93kcal/mol and -9.49 kcal/mol, respectively. Sigmar1 is an integral protein localized in mitochondrial membranes while communication between mitochondria and endoplasmic reticulum and Adiponectin receptors are known to be associated with mitochondrial function. These results suggest that 2(3), 9(10), 16(17), 23(24)-tetrakis-[N-methyl-(1-benzylpiperidin-4-yl)oxy)phthalocyaninato]zinc(II) iodide has a cytotoxic potential on cancer cells and inhibited MMP in breast cancer cells only.

Keywords: Zinc (II) phthalocyanine, aggregation, water soluble, metastatic breast cancer, mitochondrial membrane potential, molecular docking

1. Introduction

Phthalocyanines (Pcs) are applied, such as photosensitizers [1,2], liquid crystals [3,4], sensors [5,6], and catalysts [7–9] in a wide range of areas based on chemistry and nanotechnology. They have also been commonly used as pigments and dyes [10]. Metal-centered phthalocyanine (MPc) complexes are known as photoactive and can be used for photosensitization when the central metal is a diamagnetic metal atom [11,12]. Closed shell and diamagnetic ions, *i.e.*, Zn^{2+}, Ga^{3+}, and Si^{4+}, play an important role in Pc complexes with high properties, *i.e.*, high singlet oxygen generation that is crucial for photodynamic therapy (PDT) efficiency of photosensitizers [13–17]. ZnPcs are commonly studied due to a central metal ion having A full-fill shell and d^{10} configuration in optical spectra that are not complicated by additional bands, as in transition-metal Pc complexes. Having intensive red visible region absorption, high triplet yields, and efficient singlet oxygen generation make ZnPcs worthwhile photosensitizers for PDT applications or cancer treatments [17]. Aggregation behavior and solubility of phthalocyanine are significant parameters that should be examined prior to *in vitro* cancer studies. The former is observed due to the 18-π electron system of phthalocyanines and decreases their solubility property in many solvents and seriously affects their spectroscopic, photochemical, photophysical, and electrochemical properties [18,19]. It is precisely at this point that the solubility of phthalocyanines in polar or nonpolar solvents becomes important.

Citation: U. Uzuner, S. Celik-Uzuner, H.İ. Kaya, C. Akkol, M. Yilmaz, E.T. Saka, Evaluation of photocytotoxic activity of water-soluble Zn(II) phthalocyanine on cancer cells and molecular docking studies,Turk J Anal Chem, 6(2), 2024, 115–128.
https://doi.org/10.51435/turkjac.1585651

Author of correspondence: ece_t_saka@hotmail.com
Received: November 14, 2024
Accepted: December 16, 2024
Tel: +90 (462) 377 2492
Fax: +90 (462) 325 3196

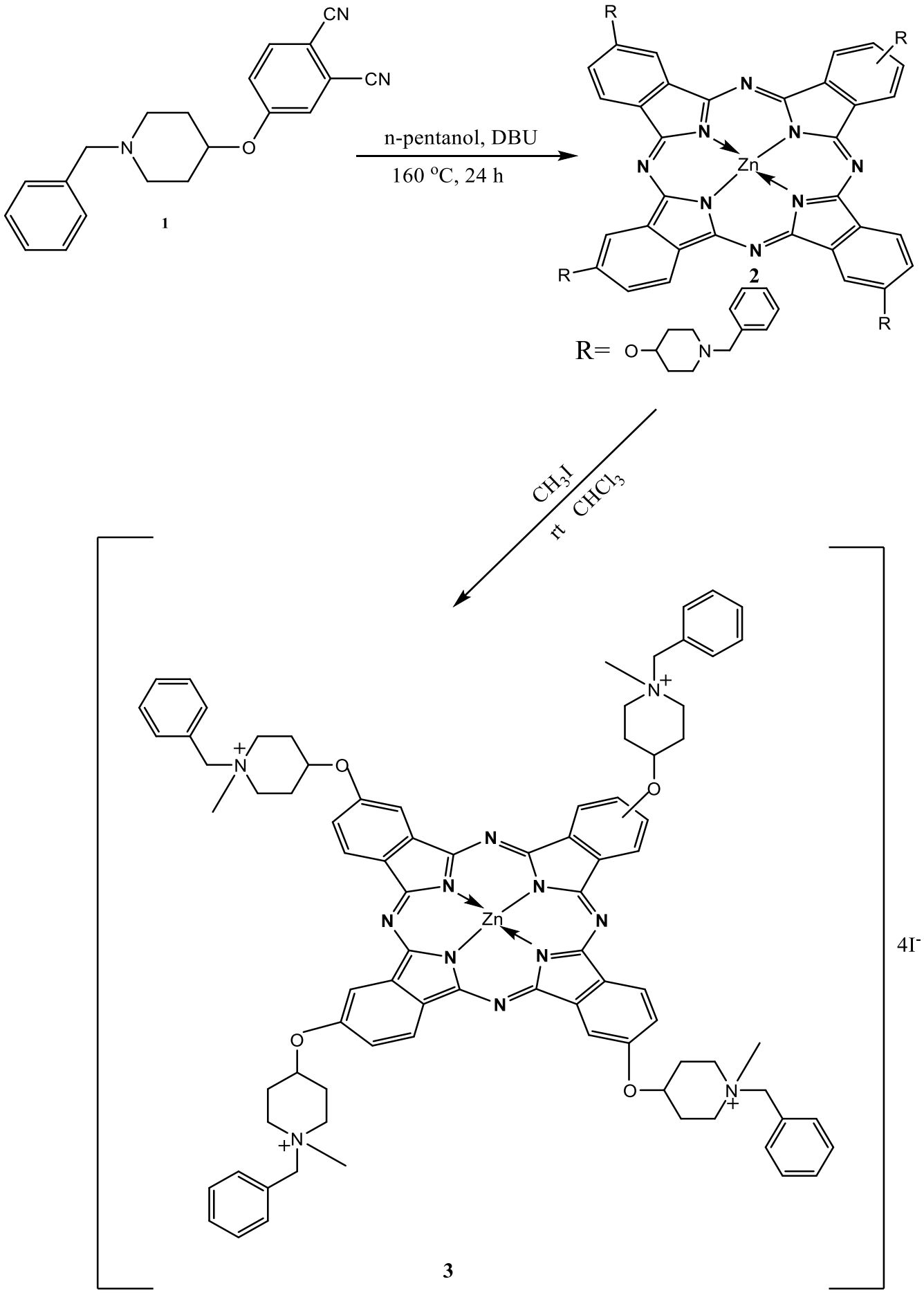

Figure 1. Synthesis of 2(3), 9(10), 16(17), 23(24)-tetrakis-[N-methyl-(1-benzylpiperidin-4-yl)oxy)phthalocyaninato]zinc(II) iodide

Solubility in water has been preferred in biological studies, in particular *in vivo* cancer studies, due to the fact that human blood itself has a hydrophilic system and the chemotherapeutics are applied intravenously [20,21].

Cancer is a common disease with a high Mortality rate around the world after cardiac diseases. Recent molecular technologies appear effective in understanding the complexity of cancer, which is to be targeted specifically for drug development. However, new candidate drugs have been in demand to overcome some limitations of current therapies such as, drug resistance, drug instability, drug insolubility, and harmful drug side effects. Therefore, innovative drug discovery technologies have focused on newly designed and more advantageous drugs. Ineffective cancer therapies can result in cancer cells that gain further molecular changes, such as metastatic characteristics. Metastasis requires aggressive cellular changes that promote increased survival, migration, and energy consumption [22]. PDT has been used to deal with metastable cancers due to the special characteristics of phthalocyanines [23]. In this work, we aimed to synthesize easily quaternerizable nitrogen atoms, including 1-benzylpiperidin-4-ol groups and characterized peripherally 2(3), 9(10), 16(17), 23(24)-tetrakis-[N-methyl-(1-benzylpiperidin-4-yl)oxy)phthalocyaninato]zinc(II) iodide to be used as a photosensitizer. Its effects on cytotoxicity and mitochondrial membrane potential were also examined in cancerous and non-cancerous cells. *In silico* target of 2(3), 9(10), 16(17), 23(24)-tetrakis-[N-methyl-(1-benzylpiperidin-4-yl)oxy) phthalocyaninato]zinc(II) iodide within the cells was screened and its inhibition potential on predicted targets was examined by *in silico* molecular docking approach.

2. Experimental

2.1. Materials

4-[(1-Benzylpiperidin-4-yloxy]phthalonitrile **(1)** [24] and 2(3), 9(10), 16(17), 23(24)-tetrakis-[1-benzylpiperidin-4-yl)oxy]phthalocyaninato zinc(II) **(2)** [25] was designed and prepared according to literature. All solvents were dried and purified as described by the reported procedure [26]. 4-Nitrophthalonitrile was purchased from commercial suppliers.

2.2. Methods

2.2.1. *Synthesis of 2(3), 9(10), 16(17), 23(24)-tetrakis-[N-methyl-(1-benzylpiperidin-4-yl) oxy)phthalocyaninato]zinc (II) iodide*

2(3), 9(10), 16(17), 23(24)-tetrakis-[1-benzylpiperidin-4-yl)oxy]phthalocyaninato zinc(II) (30 mg, 0.020 mmol) [25] was dissolved in $CHCl_3$ (3 ml), added iodomethane (3 ml), and stirred at room temperature (RT) for 3 days. The precipitated product was filtered and washed with $CHCI_3$ and hexane. Yield: 30 mg (72%), m.p.> 250 °C. FT-IR (ATR),ν/cm^{-1}: 3025 (Ar-CH), 2966–2890 (Alip.-CH), 1605, 1508, 147,1393, 1305, 1242, 1188, 1072, 1059, 1038, 978, 819, 656. UV–Vis (DMF), λ_{max}(logε) nm: 679 (4.98), 614 (5.12), 338 (4.28). ^{1}H-NMR. (DMSO), (δ:ppm): 7.78-7.60 (m, 12H, ArH), 7.53-7.38 (m, 20H, ArH), 4.70-4.55(m, 8H, CH_2-N^+), 4.47-4.28 (m, 4H, CH-O), 3.88-3.63 (m, 16H, CH_2-N^+), 3.02 (s, 12H, CH_3-N^+), 1.87-170 (m, 16H, Aliph.CH_2) ^{13}C-NMR. (DMSO), (δ:ppm): 170.13 (ArC), 165.63 (ArC), 149.56 (ArC), 148.71 (ArC), 147.25 (ArC), 135.34 (ArC), 132.18 (ArC), 130.27 (ArC), 128.66 (ArC), 127.38 (ArC), 125.78 (ArC), 125.60 (ArC), 122.17 (ArC), 120.89 (ArC), 80.23 (Aliph.CH-O), 61.35 (Aliph.CH_2-N^+), 60.02 (Aliph.CH_2-N^+), 51.30 (Aliph.CH_2-N^+), 50.25 (Aliph.CH_3-N^+), 33.82 (Aliph.CH_2), 32.05(Aliph.CH_2). Anal. Calcd for $C_{84}H_{88}ZnN_{12}O_4I_4$ (1902.6821 g/mol) C, 53.02; H, 4.66; N, 8.83, Found: C, 53.09; H, 4.68; N, 8.81; MALDI-TOF-MS m/z calc. 1902. 682; found: 344.81 $[M\text{-}4I\text{-}H_2O)]^{+4}$.

2.2.2. Cell culture

Pancreatic cancer cell line (AR42J) (ATCC Cat CRL-1492), metastatic breast cancer cell line (MDA-MB-231) (ATCC Cat HTB-26), and normal myoblast cells (Sol8) (ATCC Cat CRL-2174) were used in this study. AR42J, MDA-MB-231, and Sol8 cells were incubated in RPMI, EMEM, and DMEM media, respectively and each complete media also contained 20% fetal bovine serum and 1% Penicillin-Streptomycin antibiotics. Cells were cultured at 37°C, the normal physiological temperature of the human body, in a humidified environment with 5% CO_2 to maintain the normal rate of blood gas in the human body. After cells reached full confluency (except for Sol8 cells which are recommended to be cultured by a maximum of 80% confluency by the manufacturer as these cells can undergo cellular differentiation at the full confluent stage), cells were seeded into 96-well plates for cytotoxicity and mitochondrial assessments.

2.2.3. 2(3), 9(10), 16(17), 23(24)-Tetrakis-[N-methyl-(1-benzylpiperidin-4-yl)oxy) phthalocyaninato]zinc(II) iodide treatment and MTT cytotoxicity assay

Cells were cultured in 96-well plates as 10.000 cells per well. After they proliferated as desired, media including 2(3), 9(10), 16(17), 23(24)-tetrakis-[N-methyl-(1-benzylpiperidin-4-yl)oxy)phthalocyaninato]zinc(II) iodide at 1.5, 3, 6 and 12 micromolar was added to cells and incubated for 24 or 48 hours. Different concentrations were prepared by serial dilution in the culture media.

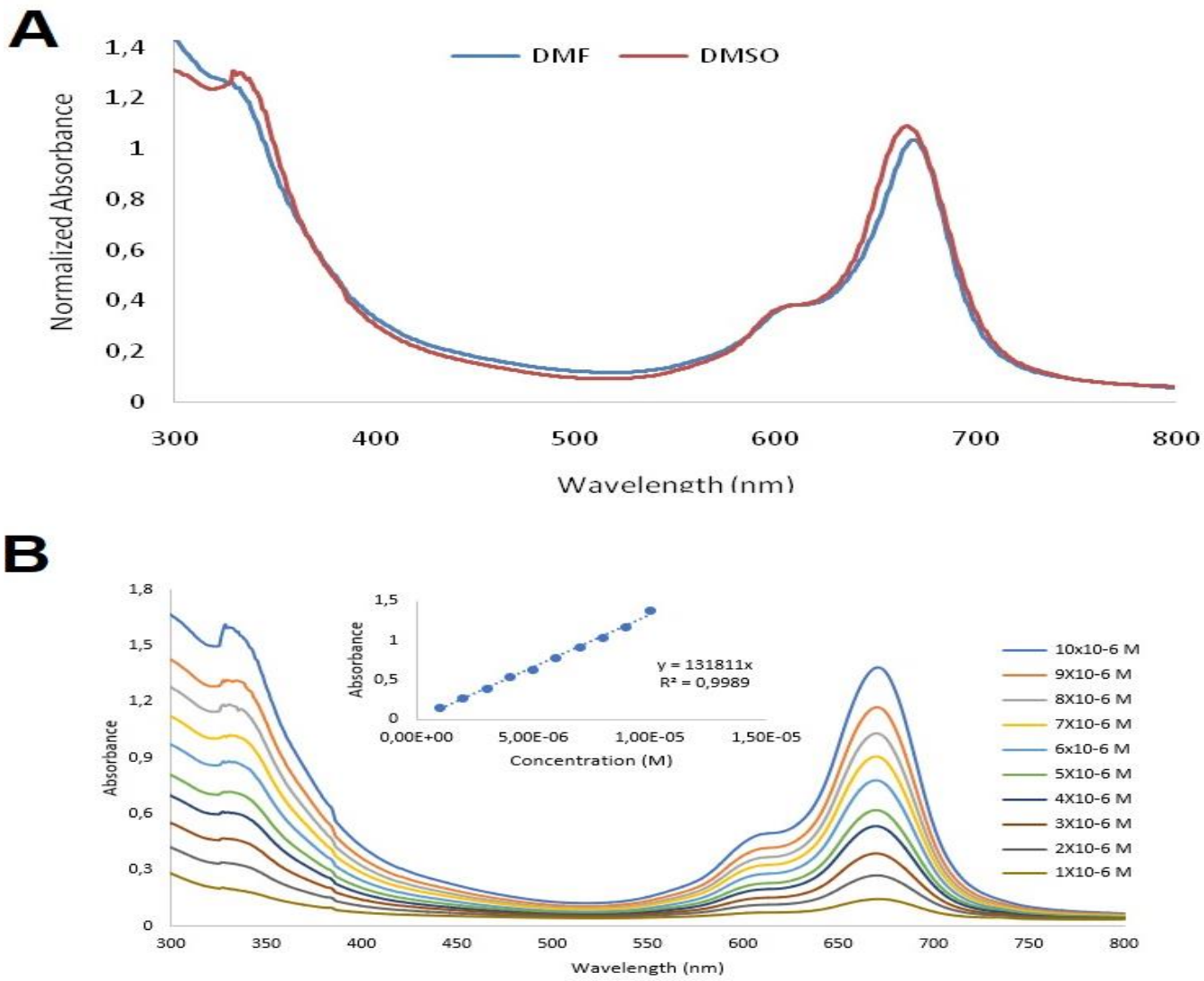

Figure 2. UV-Vis spectrum of 2(3), 9(10), 16(17), 23(24)-tetrakis-[N-methyl-(1-benzylpiperidin-4-yl)oxy)phthalocyaninato]zinc(II) iodide. A- represents two spectra of the red line is the UV-Visible spectrum of phthalocyanine in DMSO and the blue one is also the UV-Visible spectrum of phthalocyanine in DMF. B- shows the concentration effect of aggregation in DMSO with phthalocyanine between $1x10^{-6}$- $10x10^{-6}$ molar concentration.

Some cells were treated in the dark (covered by foil and incubated in a dark room) as a control group. Internal groups of cells for each experimental design were untreated and used as a control. After pre-incubation with water soluble Zn(II) phthalocyanine, cells were exposed to red light at a wavelength of 680 nm. The total irradiation dose was adjusted to 10 j/cm^2 as before [27–30]. Duration of light exposure was calculated by the formula; J = W x S (J = desired amount of light energy, W = Light power received by the sensor and S = Duration (hour) to be applied depending on desired light energy and light power). After 1 hour of exposure, cells were incubated for a further 24 hours followed by the MTT protocol [31]. For this protocol, media was removed from all the wells, wells were washed once with 1xPBS, then 190 µl fresh media (without phthalocyanine) and 10 µl MTT dye were added to each well and incubated for 2 hours at 37°C. MTT incubation was stopped by 200µl solvent addition to each well after media with MTT was removed. Wells were incubated with the solvent overnight in the dark on the shaker. The day after, absorbances were read at 570 nm using a spectrophotometer. Cell viabilities (%) were relatively calculated according to untreated cells which are considered as 100% viable.

2.2.4. *Assessment of mitochondrial membrane potential*

Cells were incubated and treated as mentioned above. Differentially, after 24h incubation with ZnPc wells were washed with 1xPBS followed by the treatment with media including $4.0x10^{-3}$M MitoTracker Red (ThermoFisher, M7512) for 45 minutes at 37°C [32]. MitoTracker treated wells were washed with 1×PBS three times and fluorescence was read at 579/599 using a microplate reader.

2.2.5. In silico target prediction for 2(3), 9(10), 16(17), 23(24)-tetrakis-[N-methyl-(1-benzylpiperidin-4-yl)oxy)phthalocyaninato]zinc(II) iodide

In silico target prediction for 2(3), 9(10), 16(17), 23(24)-tetrakis-[N-methyl-(1-benzylpiperidin-4-yl)oxy)phthalocyaninato]zinc(II) iodide was performed using the Similarity ensemble approach (SEA) [33]. The SEA approach is effective in performing analyses based on set-based chemical similarity between ligands of proteins. It is useful for quickly browsing large composite databases and generating *in silico* predictions from similarity maps by identifying cross-targets.

2.2.6. 3D structure preparation of zinc (II) phthalocyanine and target proteins and molecular docking

To evaluate the ligand-based affinity of phthalocyanine, the SDF file of 2(3), 9(10), 16(17), 23(24)-tetrakis-[N-methyl-(1-benzylpiperidin-4-yl)oxy)phthalocyaninato]zinc(II) iodide was initially created using Open Babel software [34]. Energy minimization was performed by AutoDock MGL Tools and Gasteiger charges were assigned to the compound prior to molecular docking studies [35]. The 3D structures of ADPNR1 (PDB ID: 5LXG), ADPNR2 (PDB ID: 6YX9), and Sigmar1 (PDB ID: 5HK1) were retrieved from the Protein Data Bank (www.rcsb.org). All structures were processed before molecular docking studies. Bound water molecules were initially removed from the 3D protein structures, polar hydrogens were added to each protein and eventually the structures were charged with Kollman charges before saving their pdbqt files. Grid box sizes were adjusted based on the catalytic core of each protein target to surround the amino acid domain involved in the binding active sites. For this, grid center coordinates and box size values for ADPNR1-2(3), 9(10), 16(17), 23(24)-tetrakis-[N-methyl-(1-benzylpiperidin-4-yl)oxy)phthalocyaninat]zinc(II) iodide docking was set as 23, 31 and 2,4 and the box size was 35, 35, 35. On the other hand, the related calculations were set as 12, -21, -22 and the box size was 35, 35, 35 for ADPNR2. However, the catalytic core of Sigmar1 was identified as buried into the target receptor. Therefore, we performed blind docking experiment on Sigmar1 receptor to determine the best binding pose of 2(3), 9(10), 16(17), 23(24)-tetrakis-[N-methyl-(1-benzylpiperidin-4-yl)oxy) phthalocyaninato]zinc(II) iodide. For this goal, the grid center coordinates were set as 14, 38, -36 and the dimensions of the box size value were adjusted as 50, 45, and 47. Molecular docking studies were then performed for ADPNR1 and ADPNR2 proteins using AutoDockZn software [36], whereas, targeting 2(3), 9(10), 16(17), 23(24)-tetrakis-[N-methyl-(1-benzylpiperidin-4-yl)oxy) phthalocyaninato]zinc(II) iodide compound to Sigmar1 receptor was performed using AutoDock4 [37].

2.2.7. Statistics

The fluorescence values of MMP activity were analyzed by the UNIANOVA test of SPSS software. The comparison for cell viability (%) was also performed using the UNIANOVA. The significance is considered if p value is less than 0.05. Significant levels used were $p<0.05$ (*), $p<0.01$ (**), $p<0.001$ (***) and $p<0.0001$ (****). Experiments were completed as at least three independent repeats and standard errors of the means (+/-s.e.m.) were calculated by the SPSS (Version 13) program.

3. Results and Discussion

4-[(1-Benzylpiperidin-4-yloxy]phthalonitrile **1** and 2(3), 9(10), 16(17), 23(24)-tetrakis-[1-benzylpiperidin-4-yl)oxy]phthalocyaninato zinc(II) were synthesized according to literatures, as mentioned in the material and method section [24-25]. 2(3), 9(10), 16(17), 23(24)-tetrakis-[N-methyl-(1-benzylpiperidin-4-yl)oxy)phthalocyaninato]zinc(II) iodide was synthesized by the reaction of 2(3), 9(10), 16(17), 23(24)-tetrakis-[1-benzylpiperidin-4-yl)oxy] phthalocyaninato zinc(II) with CH_3-I in $CHCl_3$ (Fig. 1). Quaternization of 2(3), 9(10), 16(17), 23(24)-tetrakis-[1-benzylpiperidin-4-yl)oxy]phthalocyaninato zinc(II) with an excess of methyl iodide in chloroform led to water soluble tetra cationic Zn(II) phthalocyanine. After the reaction contents were stirred at room temperature for 72 hours, the dark green crude product was precipitated at the bottom of the reaction vessel. The crude product was filtered and washed three times with chloroform and hexane. When looking at the infrared spectra of 2(3), 9(10), 16(17), 23(24)-tetrakis-[1-benzylpiperidin-4-yl)oxy] phthalocyaninato zinc(II) and its water-soluble derivative, it can be seen that both are similar. Both of them have aromatic, aliphatic carbon resonance peaks and do not have C≡N sharp resonance peak around 2230 cm^{-1} which is the very identical peak for 4-[(1-benzylpiperidin-4-yloxy]phthalonitrile as the starting molecule. The FT-IR spectra of 2(3), 9(10), 16(17), 23(24)-tetrakis-[N-methyl-(1-benzylpiperidin-4-yl)oxy)phthalocyaninato]zinc(II) iodide has had aromatic carbon resonance peaks at 3025 cm^{-1} and aliphatic carbon resonance peaks at 2966–2890.

The ^{1}H-NMR data of 2(3), 9(10), 16(17), 23(24)-tetrakis-[N-methyl-(1-benzylpiperidin-4-yl)oxy)phthalocyaninato]zinc(II) iodide in DMSO-d_6 showed signals due to the appearance of aromatic protons at 7.78-7.60 and 7.53-7.38 ppm. The CH_3 group of 2(3), 9(10), 16(17), 23(24)-tetrakis-[N-methyl-(1-benzylpiperidin-4-yl)oxy)phthalocyaninato]zinc(II) iodide was indicated as an singlet at 3.02 ppm.

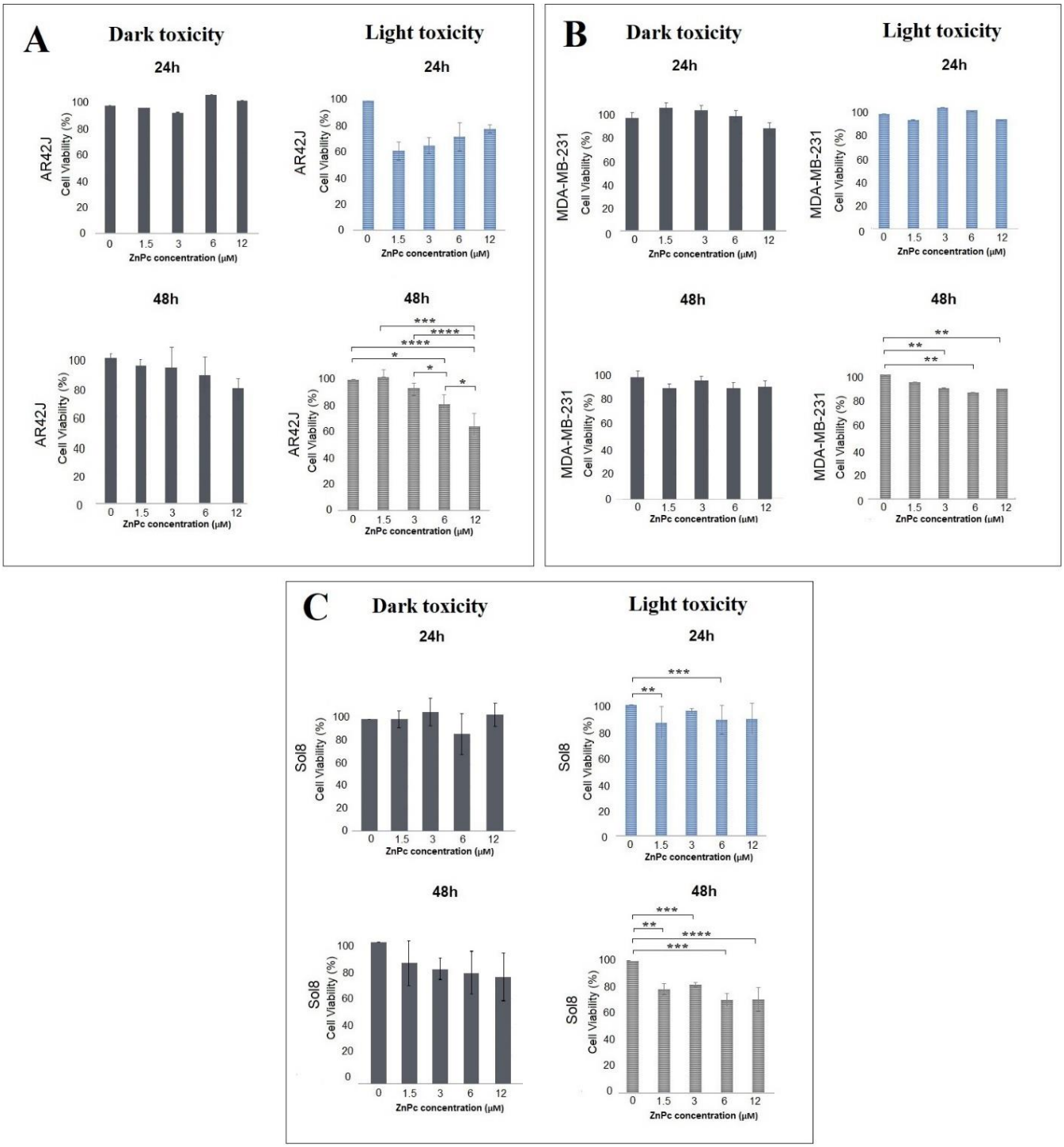

Figure 3. Cell viability 2(3), 9(10), 16(17), 23(24)-tetrakis-[N-methyl-(1-benzylpiperidin-4-yl)oxy)phthalocyaninato]zinc (II) iodidetreatment in AR42J, MDA-MB-231 and Sol8 cells. Cell percentages (%) are shown for AR42J (A), MDA-MB-231 (B), and Sol8 (C) cells after phthalocyanine treatments (0, 1.5, 3, 6, and 12μM) both for 24h (up panels)and 48h(down panels), after light (right panels) and dark (unlightened) exposure (left panels). p<0.05 (*), p<0.01 (**), p<0.001 (***) and p<0.0001 (****)

The aliphatic protons were observed at 4.70-4.55, 4.47-4.28, 3.88-3.63, and 1.87-170 ppm. The ^{13}C-NMR spectrum of the quaternary ammonium group containing zinc (II) phthalocyanine was taken in DMSO-d_6 and construed as having 21 carbon atoms in the structure. In the ^{13}C-NMR spectrum, 14 different signals for aromatic carbon atoms between 170.13 and 120.89 ppm and also 7 signals for aliphatic carbon atoms between 80.23 and 32.05 ppm comply with the proposed structure.

The molecular ion peak of 2(3), 9(10), 16(17), 23(24)-tetrakis-[N-methyl-(1-benzylpiperidin-4-yl)oxy)phthalocyaninato]zinc(II) iodide was seen at m/z=344.81 $[(M\text{-}4I\text{-}H_2O)]^{+4}$ (*S. Fig. 1*). Elemental analysis also supports the proposed structure of Zn(II) phthalocyanine. UV-Vis spectrum of 2(3), 9(10), 16(17), 23(24)-tetrakis-[N-methyl-(1-benzylpiperidin-4-yl)oxy) phthalocyaninato]zinc(II) iodide was measured in water (*S. Fig. 2*).

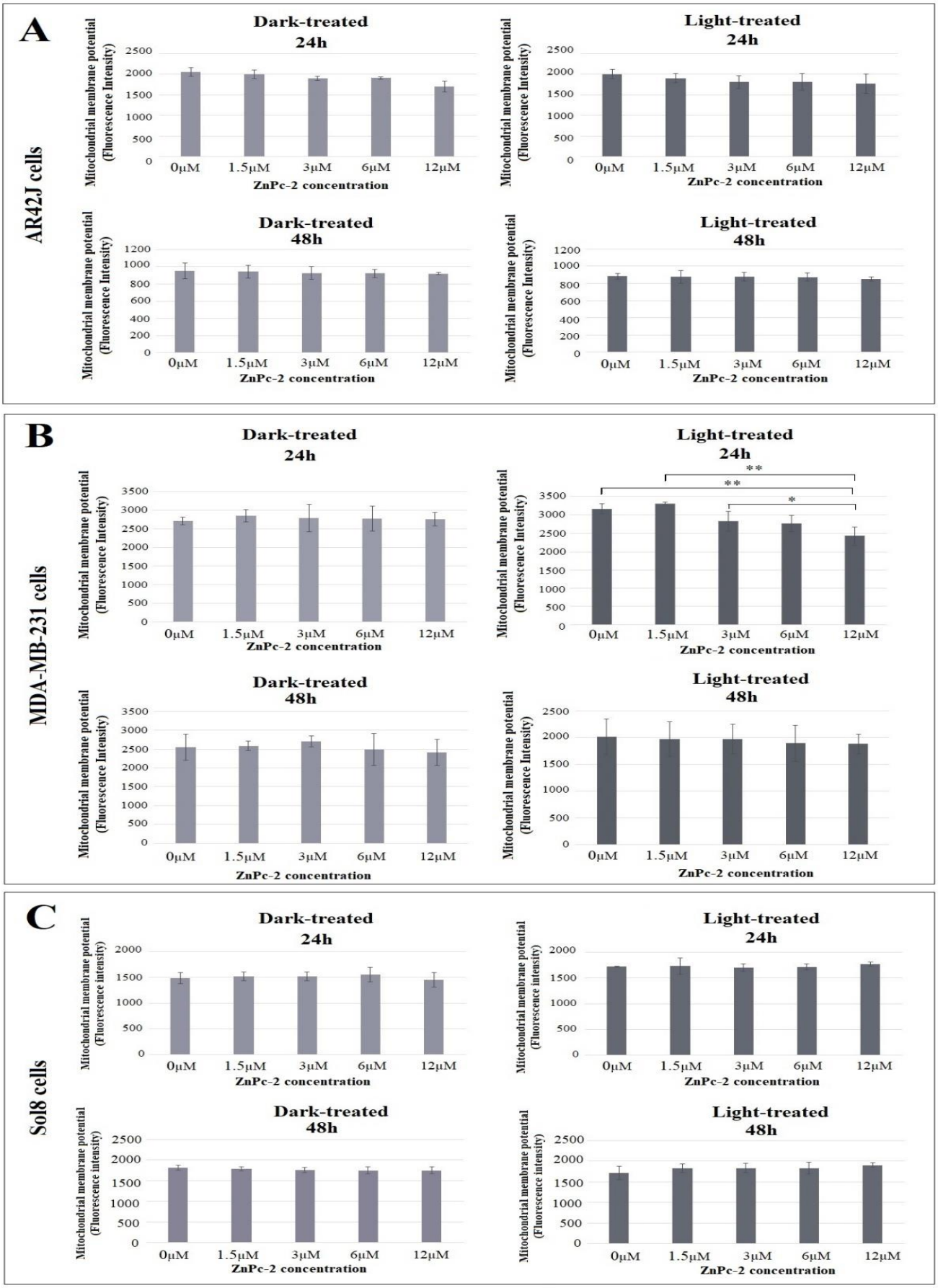

Figure 4. Mitochondrial membrane potential after phthalocyanine treatment. Mitochondrial membrane potential values were calculated in immunostaining photos by Image J software, and these are shown for AR42J (A), MDA-MB-231 (B), and Sol8 (C) cells after 24h (up panels)or 48h(down panels)treatment with different doses of phthalocyanine treatment before light exposure followed by light (right panels) or dark (unlightened) exposure (left panels). $p<0.05$ (*), $p<0.01$ (**), $p<0.001$ (***) and $p<0.0001$ (****)

Additionally, the aggregation behavior of 2(3), 9(10), 16(17), 23(24)-tetrakis-[N-methyl-(1-benzylpiperidin-4-yl)oxy) phthalocyaninato]zinc(II) iodide was measured in DMSO (Fig. 3A). Dimethyl sulfoxide (DMSO) is a dipolar aprotic solvent (μ= 3.96 D) of moderate dielectric constant (ε = 45.0) totally miscible with water, having two sites of coordination of different softness and being consequently a good solvent for cations. The UV–vis absorption spectrum of 2(3), 9(10), 16(17), 23(24)-tetrakis-[N-methyl-(1-benzylpiperidin-4-yl)oxy)phthalocyaninato]zinc(II) iodide in dry DMSO, presented in Fig. 2A, shows a peak at about 679 nm in the Q band region, with a much less intense one at 614 nm, as usually observed in organic media for a monomeric zinc(II) phthalocyanine [38–41]. The maximum absorbance at 338 nm in the Soret region is lower than that of the Q band in the visible region. This spectrum is typical of many metallophthalocyanines: the two Q and Soret bands are $\pi \rightarrow \pi^*$ transitions, $a_{1u} \rightarrow e_g$ for the Q band and $a_{2u} \rightarrow e_g$ for the Soret [42–44]. The spectrum can be totally different in pure water. The Q band maximum is much less intense than the peak in DMSO and this band looks broader because two other absorption bands are apparent as shoulders somewhat below 600 nm and at 680–690 nm. This spectrum is typical of dimeric M(II)phthalocyanines, for example, one of the Cu(II) sulfophthalocyanine [45–46]. L'Her et al. examined the influence of the concentration on the spectrum in water over a large range of concentration, from 6.4×10^{-4} M to 6.4×10^{-7} M, using cells with optical lengths from 0.1 mm to 10 cm. No evolution of the spectra reduced to ε was observed, which means that Beer's law is obeyed, and that dilution has no influence on the composition of the solution over this extended concentration range. As a consequence, these aggregates are very stable, even at the lowest concentration, and their dissociation constant cannot be estimated, unlike what has been possible for many phthalocyanines [47]. From the comparison with DMSO and water, it is evident that the zinc phthalocyanine exists as a mixture of the monomer and aggregates [48]. Additionally, solvent type effects were investigated (Fig. 2B) with different concentrations (*S. Fig. 2*) on the behavior of 2(3), 9(10), 16(17), 23(24)-tetrakis-[N-methyl-(1-benzylpiperidin-4-yl)oxy)phthalocyaninato]zinc(II) iodide.

2(3), 9(10), 16(17), 23(24)-Tetrakis-[N-methyl-(1-benzylpiperidin-4-yl)oxy) phthalocyaninato]zinc(II) iodide was then proceeded for *in vitro* biological analysis. First, its cytotoxic potential in AR42J pancreatic cancer cells, MDA-MB-231 metastatic breast cancer cells, and Sol8 normal muscle cells was evaluated. Dark treated cells (as a control group to light) were also included in the experiment. None of the conditions in the dark (at 24 or 48 hours) resulted in a significant change in cell viability (Fig. 3A–Fig. 3C, left panels). However cytotoxic effects after light exposure have been shown in AR42J cells and Sol8 at 48h with around 30% reduction (Fig. 3A and Fig. 3C, right panels). Although a reduction was detected, The IC-50 values could not be calculated. Pair-wise comparisons are performed by post-hoc test and the significant levels are shown by asterisks between the compared doses (Fig. 3A–Fig. 3C, right panels). Detailed statistical analyses for cytotoxicity after light are provided in *S. Fig. 3* (blue squares indicate significant comparisons). IC50 value for Zn(II) phthalocyanines (ZnPcs) conjugated with thiopyridinium units was determined as 20 μM in melanoma cells [49]. Octal-bromide zinc phthalocyanine (ZnPcBr8) resulted in the death of almost all (around 100%) Hep-2 (laryngeal carcinoma) cells at 24h [50]. These suggest that the effectiveness of ZnPc molecules may depend on the structure and the type of cancer cells examined. ZnPc was used to be incorporatedinto extracellular vesicules and this was found to reduce colon cancer growth over 2 weeks [51]. However, phthalocyanines can also be effectively cytotoxic regardless of light induction. A study showed that the two dyads composed of zinc(II) phthalocyanine and tin complexes were more cytotoxic in MCF-7 human breast cancer when it was treated in the darkcompared to lightwith an IC50 between 0.016 and 0.453 μM [52]. On the other hand, photodynamic therapy with zinc phthalocyanine was shown to enhance the anti-cancer effect of some common chemotherapeutics, *i.e.*,tamoxifen in breast cancer cell lines [53].

However, mitochondrial membrane potential was gradually decreased in MDA-MB-231 cells at 24 h after zinc (II) phthalocyanine treatment ($p<0.05$) (Fig. 4B)compared to both AR42J (Fig. 5A) and Sol8 cells (Fig. 5C). 48h pretreatment with 2(3), 9(10), 16(17), 23(24)-Tetrakis-[N-methyl-(1-benzylpiperidin-4-yl)oxy)phthalocyaninato]zinc(II) iodide did not induce MMP decrease as much as 24h pretreatment (Fig. 4B). Detailed statistical analyses for mitochondrial membrane potential are provided in *S. Fig. 4* (blue squares indicate significant comparisons). Representative staining for mitochondrial membrane potential after 12 μM water soluble Zn(II) phthalocyanine (after 24h) is shown in Fig. 5D. A, B, and C show Δψm values in AR42J, MDA-MB-231, and Sol8 cells, respectively. Fig. 5 shows representative fluorescence imaging of mitochondrial staining. Mitochondrial membrane potential was shown to reduce in different cancer cell lines after ZnPc compounds [54–56].

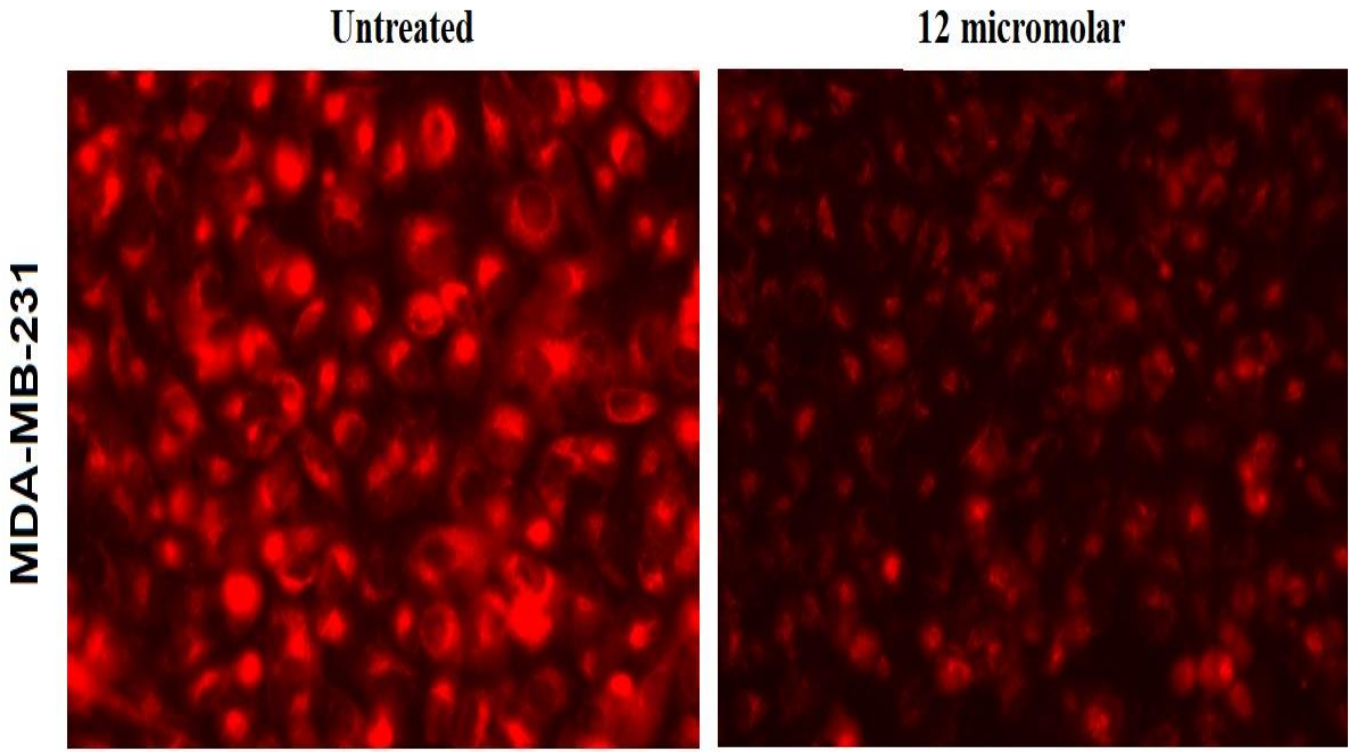

Figure 6. Representative fluorescent labeling of mitochondria by MitoTracker Red. The figure shows the staining in untreated and treated (by 12 micromolar phthalocyanine for 24 hours) followed by irradiation in MDA-MB-231 cells.

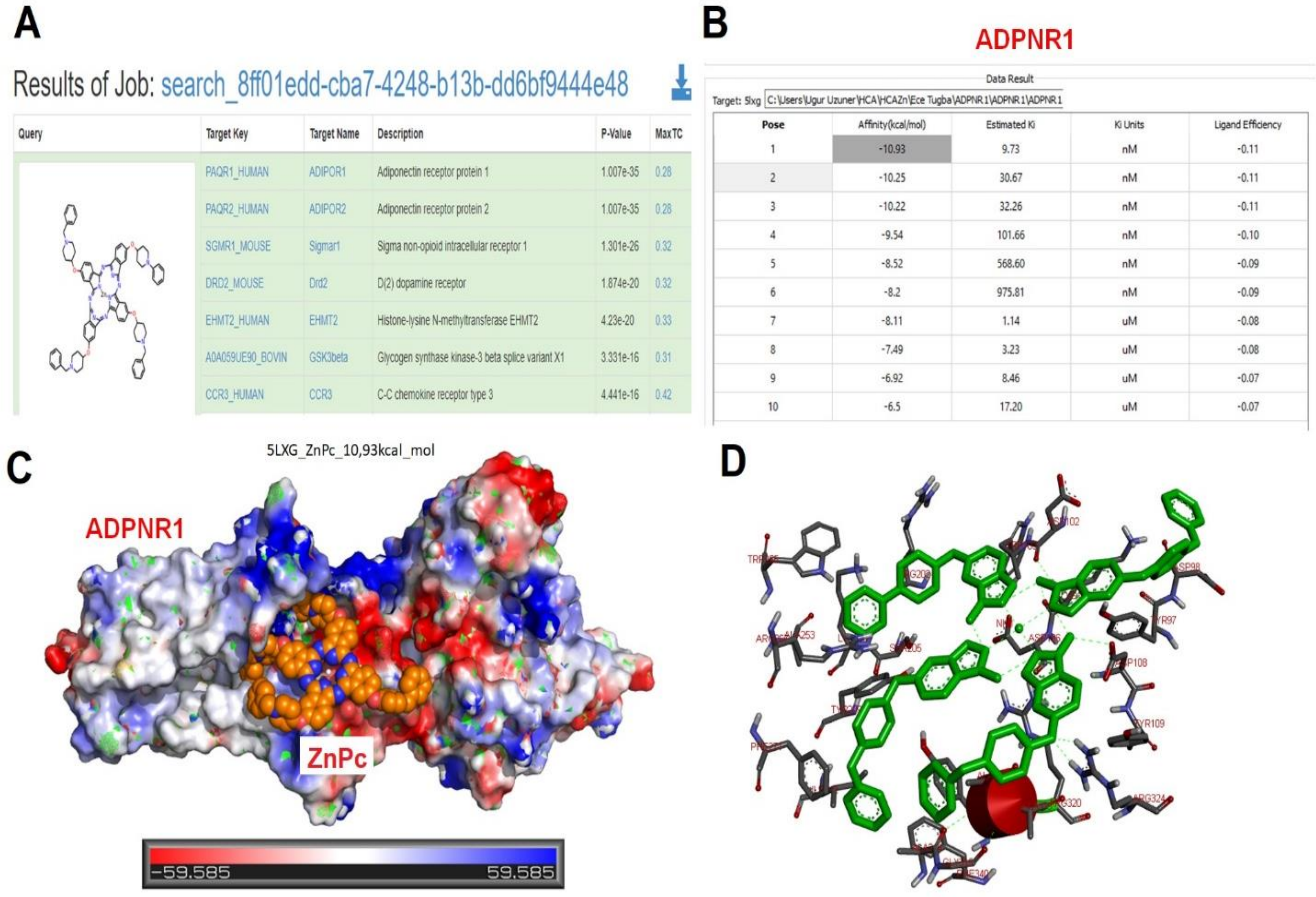

Figure 5. Target prediction of 2(3), 9(10), 16(17), 23(24)-tetrakis-[N-methyl-(1-benzylpiperidin-4-yl)oxy)phthalocyaninato]zinc(II) iodide in the cells and docking with Adiponectin Receptor 1.A shows the top 7 targets for phthalocyanine in the cells with the highest *p* values. The top three targets include 1)Adiponectin receptor 1 (ADPNR1), 2) Adiponectin receptor 2 (ADPNR2), and 3) Sigma non-opioid intracellular receptor 1 (Sigmar1). B shows 10 different poses for the docking of phthalocyanine with ADPNR1 protein by binding affinities, estimated Ki values, Ki units, and ligand efficiency. C shows the best representative of pose for docking. D shows the predicted 2D interaction map of phthalocyanine with

A

ADPNR2

Data Result

Target: 6yx9 C:\Users\Ugur Uzuner\HCA\HCAZn\Ece Tugba\ADPR2\ADPR2\ADPR2.

Pose	Affinity(kcal/mol)	Estimated Ki	Ki Units	Ligand Efficiency
1	-9.49	110.61	nM	-0.10
2	-9.25	165.85	nM	-0.10
3	-7.92	1.57	uM	-0.08
4	-6.97	7.78	uM	-0.07
5	-6.68	12.69	uM	-0.07
6	-6.41	20.02	uM	-0.07
7	-6.08	34.94	uM	-0.06
8	-6.07	35.54	uM	-0.06
9	-5.98	41.37	uM	-0.06
10	-5.12	0.18	mM	-0.05

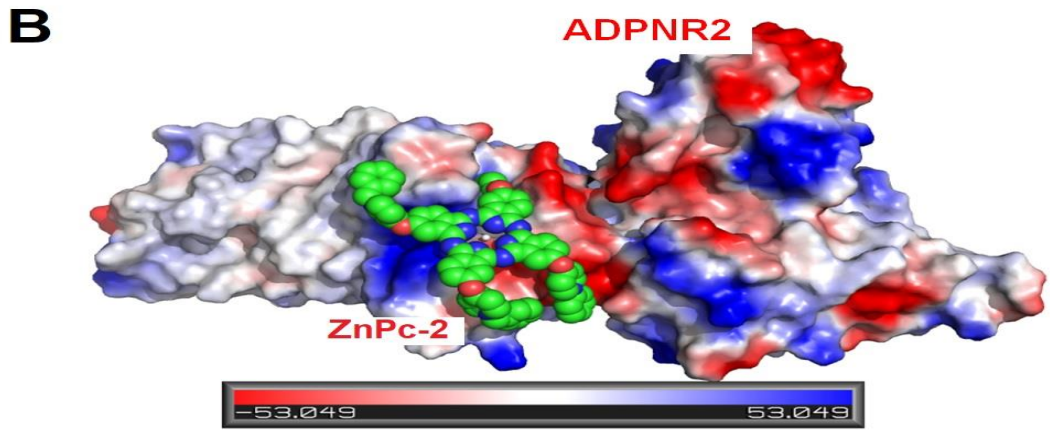

Figure 7. 2(3), 9(10), 16(17), 23(24)-Tetrakis-[N-methyl-(1-benzylpiperidin-4-yl)oxy) phthalocyaninato]zinc(II) iodide docking with Adiponectin Receptor 2 (ADPNR2).A shows 10 different poses for the docking of phthalocyanine with ADPNR2 protein by binding affinities, estimated Ki values, Ki units and ligand efficiency. B shows the best representative of pose for docking.

When potential protein or receptor targets were screened, the top three targets of 2(3), 9(10), 16(17), 23(24)-tetrakis-[N-methyl-(1-benzylpiperidin-4-yl)oxy)phthalocyaninato]zinc(II) iodide were identified as Adiponectin receptor 1 (ADPNR1), Adiponectin receptor 2 (ADPNR2) and sigma non-opioid intracellular receptor 1 (Sigmar1) proteins. *In silico* target prediction analysis were hit for the two intracellular targets for 2(3), 9(10), 16(17), 23(24)-tetrakis-[N-methyl-(1-benzylpiperidin-4-yl)oxy)phthalocyaninato]zinc(II) iodide including ADPNRs and Sigmar1 protein with the highest significance (Fig. 6A). *In silico* docking analyses were then performed for ADPNR1 (Fig. 6B–Fig. 6D). 10 different binding poses for the active domain of target proteins were analyzed (Fig. 6B) and the docking for the highest affinity along with the lowest binding energy (−10.93 kcal/mol) was modeled (Fig 6C and Fig 6D). ADPNR1 and ADPNR2 proteins are secreted from white adipose tissue [57], and mitochondrial function was dysregulated in mice lacking ADPNR1 [58]. ADPNR1 increased mitochondrial function in skeletal muscle cells [57], and it is highly associated with the regulation of glucose and lipid metabolism and with mitochondrial biogenesis [59]. However, the effect of ADPNR1 deficiency on mitochondrial protein composition has been found to be highly tissue-specific [58]. ADPNR2 was also docked with phthalocyanine and the binding affinity of 2(3), 9(10), 16(17), 23(24)-tetrakis-[N-methyl-(1-benzylpiperidin-4-yl)oxy) phthalocyaninato]zinc(II) iodide to ADPNR2 (–9.49 kcal/mol) (Fig. 7A) was found to be less than the binding affinity to ADPNR1 (–10.93 kcal/mol). Both ADPNRs are able to bind metals in particular zinc (from the Uniprot database) which are included in the core structure of synthesized water soluble Zn(II) phthalocyanine. ADPNR1/ADPNR2 were reported to recover non-alcoholic hepatitis and fibrosis by their roles in between ER and mitochondria communication [60].

We then analyzed the third *in silico* target of phthalocyanine, Sigmar1. The best pose for Sigmar1 was detected with the lowest binding energy as –13.07 kcal/mol (Fig. 8A). The docking of this pose was modeled (Fig 8B–Fig 8C). Sigma receptor 1 (Sigmar1) is a chaperone significantly localized in the mitochondrial membrane of cardiomyocytes [61], but Sigmar1 is expressed in a range of tissues so that it is considered as having housekeeping function in each cell type [61,62].

A

Load Data | C:\Users\Ugur Uzuner\HCA\HCAZn\Ece Tugba\5HK1\5hk1\5hk1 | Results File

Data Result

Target: 5hk1

Pose	Affinity(kcal/mol)	Estimated Ki	Ki Units	Ligand Efficiency
1	-13.07	0.26	nM	-0.14
2	-11.45	4.05	nM	-0.12
3	-11.06	7.82	nM	-0.12
4	-11.03	8.22	nM	-0.11
5	-9.31	149.88	nM	-0.10
6	-9.14	199.68	nM	-0.10
7	-7.79	1.95	uM	-0.08
8	-7.31	4.38	uM	-0.08
9	-6.56	15.54	uM	-0.07

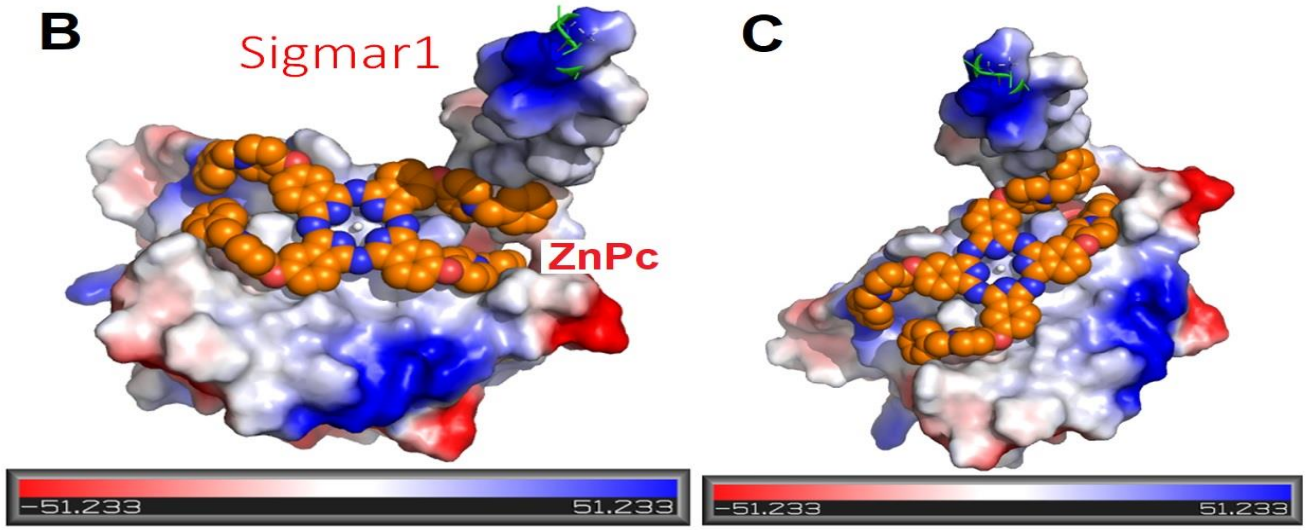

Figure 8. 2(3), 9(10), 16(17), 23(24)-Tetrakis-[N-methyl-(1-benzylpiperidin-4-yl)oxy) phthalocyaninato]zinc(II) iodide docking with Sigmar1 protein.A shows 10 different poses for the docking of phthalocyanine with Sigmar1 protein by binding affinities, estimated Ki values, Ki units, and ligand efficiency. B and C show the best representative of the pose for docking from different angles.

This is also localized in the cell membrane and nuclear membrane [63]. The Sigmar-1 upregulation was found to be associated with enhanced membrane invasiveness [62]. Sigmar1 receptor is required for proper respiration in mitochondria [61] and also has a role in the communication between mitochondria and endoplasmic reticulum [63]. The cells with knock-downed Sigmar1 showed an increase in cell death rate suggesting its association with cell survival [63]. Deficiency in Sigmar1 is associated with a range of diseases such as neurodegenerative diseases, cancer, and cardiovascular diseases [62]. Clinical studies showed that Sigmar1 is abundant in breast cancer patients [64]. Its increase has also been detected in other cancers including liver, colon, prostate, and lung [62], whereas the change in the level of Sigmar1 was not significant inpatients with pancreatic cancer compared to healthy controls [63]. Current molecular docking studies show that 2(3), 9(10), 16(17), 23(24)-tetrakis-[N-methyl-(1-benzylpiperidin-4-yl)oxy)phthalocyaninato]zinc(II) iodide exhibits high binding affinity to the intramembrane interaction surface of the Sigmar1 trimeric complex, thereby causing inactivation of the sigmar1 complex, which is essential for the maintenance of mitochondrial functions.

Both Sigmar1 and ADPNR1 play key roles during the maintenance of mitochondrial function. Mitotracker red dye has been used for confirmation of Sigmar1 localization [60] as well as mitochondrial function mediated by Sigmar1 [63,65]. Sigmar1 and ADPNR genes are located in 9p13.3 and 3q27.3, respectively (from Genecards). The genome of MDA-MB-231 cells is reported as in the triploid range with the absence of chromosomes 8 and 15 by the manufacturer (ATCC), however AR42J cells are in normal diploid range with specific gene expression changes. Therefore, the levels of proteins in the examined cells are expected to be different from each other. The genomic differences between cells may suggest the variation of mitochondrial membrane potential changed by phthalocyanine. However, further investigation is required for revealing the profiles of gene expression levels in detail.

Therefore, an ultimate phthalocyanine molecule might be an effective photosensitizer that naturally

gathers in mitochondria [66]. Targeting mitochondria has been used to enhance the efficacy of photodynamic therapy [67]. Mitochondrial membrane potential (Δψm) (MMP) is an indicator of mitochondrial function. Δψm is associated with the role of mitochondria in apoptosis, and its decrease has been shown to be induced by insufficient substrates for the mitochondria, disruption in respiration, or separation of the inner membrane [68]. However, mitochondrial membrane potential has been suggested not to be an early event in the apoptosis [69]. Mitochondrial activity was found to increase after radiation treatment [70]. Some cytotoxic conditions, such as radiation, may not be associated with an increase in cell death detected by metabolic viability assays including MTT [70]. In this study, results suggest conditions for targeting mitochondrial activity by membrane potential in metastatic breast cancer only which is not correlated with cytotoxicity assessed by MTT assay. We previously showed that a silicon phthalocyanine molecule was highly cytotoxic in AR42J cells after 24h, but not in Sol8 cells, and IC50s were calculated for each cell line [27], however 2(3), 9(10), 16(17), 23(24)-tetrakis-[N-methyl-(1-benzylpiperidin-4-yl)oxy)phthalocyaninato]zinc(II) iodide was not cytotoxic in the same conditions. The critical function of Zn is that it does not quench the ability of phthalocyanine to form ROS upon irradiation. The high doses of phthalocyanine (with prolonged incubation time points) may induce cytotoxicity with calculable IC50 values which represent the effective dose to kill half of the cell population.

4. Conclusion

In this study, 2(3), 9(10), 16(17), 23(24)-tetrakis-[N-methyl-(1-benzylpiperidin-4-yl)oxy) phthalocyaninato]zinc(II) iodide was synthesized and characterized with FT-IR, UV-Vis and mass spectra and elemental analysis. Aggregation is an important factor for phthalocyanine compounds because it prevents the usage of phthalocyanine in many application areas. Aggregation of 2(3), 9(10), 16(17), 23(24)-tetrakis-[N-methyl-(1-benzylpiperidin-4-yl)oxy) phthalocyaninato]zinc(II) iodide was also investigated in different solvents using UV-spectra to examine changes in the Q and B bands. This study indicates that 2(3), 9(10), 16(17), 23(24)-tetrakis-[N-methyl-(1-benzylpiperidin-4-yl)oxy)phthalocyaninato]zinc(II) iodide has an inhibitory effect on mitochondrial,particularly in MDA-MB-231 metastatic breast cancer cells. 2(3), 9(10), 16(17), 23(24)-Tetrakis-[N-methyl-(1-benzylpiperidin-4-yl)oxy) phthalocyaninato]zinc(II) iodide was cytotoxic to all cells at the different conditions experienced. The possible cellular targets of 2(3), 9(10), 16(17), 23(24)-tetrakis-[N-methyl-(1-benzylpiperidin-4-yl)oxy)phthalocyaninato]zinc(II) iodide were predicted as Sigmar1 and Adiponectin receptors by in silico analysis. These proteins are associated with mitochondrial structure and activity. These results are required to be detailed by more comprehensive molecular studies within the cells.

Acknowledgment

This study was supported by the 2209-A project of TUBITAK (Scientific and Technological Research Council of Turkey) (Project ID: 1919B012106704).

Funding Information:

2209-A project of TUBITAK (Scientific and Technological Research Council of Turkey) (Project ID: 1919B012106704).

Declaration of interests

The authors declare that they have no known competing financial interests or personal relationships that could have appeared to influence the work reported in this paper.

References

[1] B. Ertem, H. Yalazan, O. Gungor, G. Sarkı, M. Durmus, E.T. Saka, H. Kantekin, Synthesis, structural characterization, and investigation on photophysical and photochemical features of new metallophthalocyanines, J Lumin, 204, 2018, 464–471.

[2] E.T. Saka, K. Tekintas, Light driven photodegradation of 4-nitrophenol with novel Co and Cu phthalocyanine in aqueous media, J Mol Struct, 1215, 2020, 128189.

[3] G. Onsal, Improvement of the dielectric and electro-optic properties of phthalocyanine-and quantum dot-doped nematic liquid crystals under UV illumination, J Electron Mater, 51, 2022, 3820–3830.

[4] Z.J. Comeau, R.R. Cranston, H.R. Lamontagne, C.S. Harris, A.J. Shuhendler, B.H. Lessard, Surface engineering of zinc phthalocyanine organic thin-film transistors results in part-per billion sensitivity towards cannabinoid vapor, Commun Chem, 5, 2022, 178–184.

[5] K. Rytel, K. Kedzierski, B. Barszcz, A. Biadasz, L. Majchrzycki, D. Wrobel, The influence of zinc phthalocyanine on the formation and properties of multiwalled carbon nanotubes thin films on the air–solid and air–water interface, J Mol Liq, 350, 2022, 118548.

[6] V. Ivanova, D. Klyamer, P. Krasnov, E.N. Kaya, I. Kulu, S.T. Kostakoglu, M. Durmus, T. Basova, Hybrid materials based on pyrene-substituted metallo phthalocyanines as sensing layers for ammonia detection: Effect of the number of pyrene substituents, Sens Actuators B Chem, 375, 2023, 132843.

[7] A. Sukhikh, D. Klyamer, D. Bonegardt, P. Popovetsky, P. Krasnov, T. Basova, Tetrafluorosubstituted titanyl

phthalocyanines: Structure of single crystals and phase transition in thin films, Dyes and Pigments, 231, 2024, 112391.
[8] E.T. Saka, N. Kahriman, (E)-4-(4-(3-(2-fluoro-5 (trifluoromethyl)phenyl)acryloyl)phenoxy)Substituted Co(II) and Cu(II) phthalocyanines and their catalytic activities on the oxidation of phenols, J Organomet Chem, 895, 2019, 48-58.
[9] E.T. Saka, Z. Bıyıklıoglu, H. Kantekin, Microwave-assisted synthesis and characterization of Co(II) phthalocyanine and investigation of its catalytic activity on 4-nitrophenol oxidation, Turk J Chem, 38, 2014, 1166.
[10] H. Yalazan, C. Akkol, E.T. Saka, H. Kantekin, Investigation of photocatalytic properties of cobalt phthalocyanines on benzyl alcohol photoxidation, Appl Organomet Chem, 37, 2023, e6975.
[11] E.T. Saka, H. Yalazan, Z. Bıyıklıoglu, H. Kantekin, K. Tekintas, Synthesis, aggregation, photocatalytical and electrochemical properties of axially 1-benzylpiperidin-4-oxy units substituted silicon phthalocyanine, J Mol Struct, 1199, 2020, 126994.
[12] E. Ben-Hur, M. Green, A. Prager, R. Kol, I. Rosenthal, Phthalocyanine Photosensitization of Mammalian Cells: Biochemical and Ultrastructural Effects, Photochem Photobiol, 4, 1987, 651.
[13] I.J. MacDonald, T.J. Dougherty, Basic principles of photodynamic therapy, J Porphyrins Phthalocyanines, 5, 2001, 105.
[14] H. Ali, J.E. van Lier, Metal complexes as photo-and radiosensitizers, Chem Rev, 99, 1999, 2379.
[15] R. Bonnett, Photosensitizers of the porphyrin and phthalocyanine series for photodynamic therapy, Chem Soc Rev, 24, 1995, 19.
[16] A.C. Tedesco, J.C.G. Rotta, C.N. Lunardi, Synthesis, Photophysical and Photochemical Aspects of Phthalocyanines for Photodynamic Therapy, Curr Org Chem, 7, 2003, 187.
[17] C. Göl, M. Durmus, Investigation of photophysical, photochemical and bovine serum albumin binding properties of novel water-soluble zwitterionic zinc phthalocyanine complexes, Synth Met, 162, 2012, 605.
[18] A. Gunsel, A. Yıldırım, P. Taslimi, Y. Erden, T. Taskın Tok, H. Piskin, A.T. Bilgicli, I. Gulcin, M. N. Yarasir, Cytotoxicity effects and biochemical investigation of novel tetrakis phthalocyanines bearing 2-thiocytosine moieties with molecular docking studies, Inorg Chem Commun, 138, 2022, 109263.
[19] D. D. Dominguez, A.W. Snow, J.S. Shirk, R.G.S. Pong, Role of Structural Factors in the Nonlinear Optical Properties of Phthalocyanines and Related Compounds, J Porphyrins Phthalocyanines, 5, 2002, 581.
[20] N. Masilela, T. Nyokong, The synthesis and photophysical properties of water soluble tetrasulfonated, octacarboxylated and quaternised 2,(3)-tetra-(2 pyridiloxy) Ga phthalocyanines, Dyes Pigments, 84, 2010, 242.
[21] S. Wei, J. Zhou, D. Huang, X. Wang, B. Zhang, J. Shen, Synthesis and Type I/Type II photosensitizing properties of a novel amphiphilic zinc phthalocyanine, Dyes Pigments, 71, 2006, 61.
[22] S. Aggarwal, L. Gabrovsek, L.K. Langeberg, M. Golkowski, S. Ong, F.D. Smith, J.D. Scott, Depletion of dAKAP1–protein kinase A signaling islands from the outer mitochondrial membrane alters breast cancer cell metabolism and motility, J Biol Chem, 294(9), 2019, 3152.
[23] C. Sari, I. Degirmencioglu, F. Celep, Synthesis and characterization of novel Schiff base silicon (IV) phthalocyanine complex for photodynamic therapy of breast cancer cell lines, Photodiagnosis Photodyn Ther, 42, 2023, 103504.
[24] E.T. Saka, Z. Biyiklioglu, Co(II) and Fe(II) phthalocyanines: synthesis, investigation of their catalytic activity towards phenolic compounds and electrochemical behaviour, Appl Organomet Chem, 29, 2015, 392.
[25] G. Dilber, M. Durmus, H. Kantekin, Investigation of the photophysical and photochemical behavior of substituted zinc phthalocyanines and their water-soluble quaternized derivatives, Turk J Chem, 41, 2017, 917.
[26] D.D. Perrin, W.L.F. Armarego, Purification of Laboratory Chemicals, 1989, Oxford, PergamonPres.
[27] H.İ. Kaya, C. Boguslu, E. Kabak, C. Akkol, E.T. Saka, S.C. Uzuner, The effect of silicon phthalocyanine on cell death and mitochondrial membrane potential in pancreatic cancer cells, Turk J Anal Chem, 4(2), 2022, 111.
[28] J. Schmidt, W. Kuzyniak, J. Berkholz, G. Steinemann, R. Ogbodu, B. Hoffmann, G. Nouailles, A.G. Gurek, B. Nitzsche, M. Höpfner, Novel zinc- and silicon-phthalocyanines as photosensitizers for photodynamic therapy of cholangiocarcinoma, Int J Mol Med, 42(1), 2018, 534.
[29] A.R. Simioni, F.L. Primo, A.C. Tedesco, Silicon(IV) phthalocyanine-loaded-nanoparticles for application in photodynamic process, J Laser Appl, 24(1), 2012, 012004.
[30] A. Nalçaoğlu, C. Sarı, I. Degirmencioglu, F. Celep Eyuboglu, Novel piperazine-substituted silicon phthalocyanines exert anti-cancer effects against breast cancer cells, Photodiagnosis Photodyn Ther, 37, 2022, 102734.
[31] U. Cakmak, F. Oz-Tuncay, S. Basoglu-Ozdemir, E. Ayazoglu-Demir, I. Demir, A. Colak, S. Celik-Uzuner, S.S. Erdem, N. Yildirim, Synthesis of hydrazine containing piperazine or benzimidazole derivatives and their potential as α-amylase inhibitors by molecular docking, inhibition kinetics and in vitro cytotoxicity activity studies, Med Chem Res, 30(10), 2021, 1886.
[32] S.C. Uzuner, E. Birinci, S. Tetikoğlu, C. Birinci, S. Kolaylı, Distinct Epigenetic Reprogramming, Mitochondrial Patterns, Cellular Morphology, and Cytotoxicity after Bee Venom Treatment, Recent Pat Anticancer Drug Discov, 16(3), 2021, 377.
[33] M.J. Keiser, B.L. Roth, B.N. Armbruster, P. Ernsberger, J.J. Irwin, B.K. Shoichet, Relating protein pharmacology by ligand chemistry, Nat Biotechnol, 25(2), 2007, 197–206.
[34] N.M. O'Boyle, M. Banck, C.A. James, C. Morley, T. Vandermeersch, G.R. Hutchison, Open Babel: An open chemical toolbox, J Cheminform, 3(1), 2011, 33.
[35] J. Eberhardt, D. Santos-Martins, A.F. Tillack, S. Forli, AutoDock Vina 1.2.0: New Docking Methods, Expanded Force Field, and Python Bindings, J Chem Inf Model, 61(8), 2001, 3891.
[36] D. Santos-Martins, S. Forli, M.J. Ramos, A.J. Olson, AutoDock4Zn: An Improved AutoDock Force Field for Small-Molecule Docking to Zinc Metalloproteins, J Chem Inf Model, 54(8), 2014, 2371.
[37] G.M. Morris, R. Huey, W. Lindstrom, M.F. Sanner, R.K. Belew, D.S. Goodsell, A.J. Olson, AutoDock4 and AutoDockTools4: Automated docking with selective receptor flexibility, J Comput Chem, 30(16), 2009, 2785.
[38] M. Durmuş, H. Yaman, C. Göl, V. Ahsen, T. Nyokong, Water-soluble quaternized mercaptopyridine-substituted zinc-phthalocyanines: Synthesis, photophysical, photochemical and bovine serum albumin binding properties, Dyes Pigments, 91, 2011, 153.
[39] V. Çakir, D. Çakir, M. Pişkin, M. Durmuş, Z. Biyiklioglu, New peripherally and non-peripherally tetra-substituted water soluble zinc phthalocyanines: Synthesis, photophysics and photochemistry, J Organomet Chem, 783, 2015, 120-129.
[40] C. Uslan, B.Ş. Sesalan, M. Durmuş, Synthesis of new water-soluble phthalocyanines and investigation of their photochemical, photophysical and biological properties, J Photochem Photobiol A Chem, 235, 2012, 56-64.
[41] E.T. Saka, C. Göl, M. Durmus, H. Kantekin, Z. Biyiklioglu, Photophysical, photochemical and aggregation behavior of novel peripherally tetra-substituted phthalocyanine derivatives, J Photochem Photobiol A Chem, 241, 2012, 67-78.
[42] L. Edwards, M. Gouterman, Porphyrins: XVI. Vapor absorption spectra and redox reactions: Octalkylporphins, J Mol Spectrosc, 35, 1970, 90-109.

[43] N. El Khatib, B. Boudjema, M. Maitrot, H. Chermette, L. Porte, Electronic structure of zinc phthalocyanine, Can J Chem, 66, 1988, 1087–1095.
[44] T. Nyokong, Z. Gasyna, M.J. Stillman, Analysis of the Absorption and Magnetic Circular Dichroism Spectra of Zinc Phthalocyanine and the 7-Cation-Radical Species [ZnPc(-1)]+, Inorg Chem, 26, 1987, 1087–1095.
[45] K. Bernauer, S. Fallab, Helv. Phtalocyanine in wässeriger Lösung I, Helv Chim Acta, 44, 1961, 1287-1292.
[46] M.J. Stillman, T. Nyokong, Absorption and Magnetic Circular Dichroism Spectral Properties of Phthalocyanines, Editors: C.C. Leznoff, A.B.P. Lever, 1989, New York, VCH.
[47] A.W. Snow, Phtalocyanine Aggregation, The Porphyrin Handbook, Editors: K.M. Kadish, K.M. Smith, R. Guilard, Academic Press, 2003, Amsterdam, Academic Press.
[48] M. L'Her, O. Göktuğ, M. Durmuş, V. Ahsen, A water soluble zinc phthalocyanine: physicochemical, electrochemical studies and electropolymerization, Electrochim Acta, 213, 2016, 655-662.
[49] K.A.D.F. Castro, J.A. Prandini, J.C. Biazzotto, J.P.C. Tome, R.S. da Silva, L.M.O. Lourenço, The Surprisingly Positive Effect of Zinc-Phthalocyanines with High Photodynamic Therapy Efficacy of Melanoma Cancer, Front Chem, 10, 2022, 82716.
[50] E.P.O. Silva, E.D. Santos, C.S. Gonçalves, M.A.G. Cardoso, C.P. Soares, M. Beltrame Jr, Zinc phthalocyanine-conjugated with bovine serum albumin mediated photodynamic therapy of human larynx carcinoma, Laser Phys, 26, 2016, 105601.
[51] P. Lara, R.V. Huis in 't Veld, C. Jorquera-Cordero, A.B. Chan, F. Ossendorp, L.J. Cruz, Zinc-Phthalocyanine-Loaded Extracellular Vesicles Increase Efficacy and Selectivity of Photodynamic Therapy in Co-Culture and Preclinical Models of Colon Cancer, Pharmaceutics, 13, 2021, 1547.
[52] I. Toubia, C. Nguyen, S. Diring, M. Pays, E. Mattana, P. Arnoux, C. Frochot, M.G. Bobo, M. Kobeissi, F. Odobel, Study of Cytotoxic and Photodynamic Activities of Dyads Composed of a Zinc Phthalocyanine Appended to an Organotin, Pharmaceuticals, 14, 2021, 413.
[53] N. Rajabi, F. Mohammadnejad, M.A. Doustvandi, M.A. Shadbad, M. Amini, H. Tajalli, A. Mokhtarzadeh, E. Baghbani, N. Silvestris, B. Baradaran, Photodynamic therapy with zinc phthalocyanine enhances the anti-cancer effect of tamoxifen in breast cancer cell line: Promising combination treatment against triple-negative breast cancer?, Photodiagnosis Photodyn Ther, 41, 2023, 103212.
[54] Y. Ge, X. Weng, T. Tian, F. Ding, R. Huang, L. Yuan, J. Wu, T. Wang, P. Guo, X. Zhou, A mitochondria-targeted zinc(ii) phthalocyanine for photodynamic therapy, RSC Adv, 3, 2013, 12839.
[55] J. Shao, J. Xue, Y. Dai, H. Liu, N. Chen, L. Jia, J. Huang, Inhibition of human hepatocellular carcinoma HepG2 by phthalocyanine photosensitizer PHOTOCYANINE: ROS production, apoptosis, cell cycle arrest, Eur J Cancer, 48, 2012, 2086.
[56] B.F. Perrin Tamietti, A.H.A. Machado, M. Maftoum Costa, N.S. da Silva, A.C. Tedesco, C. Pacheco Soares, Analysis of Mitochondrial Activity Related to Cell Death after PDT with AlPCS4, Photomed Laser Surg, 25, 2007, 2040.
[57] M. Okada-Iwabu, M. Iwabu, T. Kadowaki, Drug development research for novel adiponectin receptor-targeted antidiabetic drugs contributing to healthy longevity, Diabetol Int, 10, 2019, 237.
[58] M.E. Pepin, C. Koentges, K. Pfeil, J. Gollmer, S. Kersting, S. Wiese, M.M. Hoffmann, K.E. Odening, C. Mühlen, P. von zur Diehl, P. Stachon, D. Wolf, A.R. Wende, C. Bode, A. Zirlik, H. Bugger, Front Endocrinol, 10, 2019, 872.
[59] M. Iwabu, T. Yamauchi, M. Okada-Iwabu, K. Sato, T. Nakagawa, M. Funata, M. Yamaguchi, S. Namiki, R. Nakayama, M. Tabata, H. Ogata, N. Kubota, I. Takamoto, Y.K. Hayashi, N. Yamauchi, H. Waki, M. Fukayama, I. Nishino, K. Tokuyama, T. Kadowaki, Adiponectin and AdipoR1 regulate PGC-1α and mitochondria by Ca^{2+} and AMPK/SIRT1, Nature, 464, 2010, 1313–1319.
[60] H. Xu, Q. Zhao, N. Song, Z. Yan, R. Lin, S. Wu, L. Jiang, S. Hong, J. Xie, H. Zhou, R. Wang, X. Jiang, AdipoR1/AdipoR2 dual agonist recovers nonalcoholic steatohepatitis and related fibrosis via endoplasmic reticulum-mitochondria axis, Nat Commun, 11, 2020, 5807.
[61] C.S. Abdullah, R. Aishwarya, S. Alam, N.S. Remex, M. Morshed, S. Nitu, S. Miriyala, M. Panchatcharam, B. Hartman, J. King, M. Alfrad Nobel Bhuiyan, J. Traylor, C.G. Kevil, A.W. Orr, S. Md. Bhuiyan, The molecular role of Sigmar1 in regulating mitochondrial function through mitochondrial localization in cardiomyocytes, Mitochondrion, 62, 2022, 159-175.
[62] R. Aishwarya, C.S. Abdullah, M. Morshed, N.S. Remex, Md. S. Bhuiyan, Sigmar1's Molecular, Cellular, and Biological Functions in Regulating Cellular Pathophysiology, Front Physiol, 12, 2021, 705575.
[63] T. Hayashi, T.P. Su, Sigma-1 Receptor Chaperones at the ER-Mitochondrion Interface Regulate Ca2+ Signaling and Cell Survival, Cell, 131, 2007, 596-610.
[64] J. Simony-Lafontaine, M. Esslimani, E. Bribes, S. Gourgou, N. Lequeux, R. Lavail, J. Grenier, A. Kramar, P. Casellas, Immunocytochemical assessment of sigma-1 receptor and human sterol isomerase in breast cancer and their relationship with a series of prognostic factors, Br J Cancer, 82, 2000, 1958–1966.
[65] D. Magouliotis, V. Tasiopoulou, K. Dimas, N. Sakellaridis, D. Zacharoulis, Gene expression profile of sigma-1 (s1R) and sigma-2 (s2R) receptors in pancreatic cancer, HPB, 20, 2018, S564.
[66] S.M. Mahalingam, J.D. Ordaz, P.S. Low, Targeting of a Photosensitizer to the Mitochondrion Enhances the Potency of Photodynamic Therapy, ACS Omega, 3, 2018, 6066–6074.
[67] A.P. Thomas, L. Palanikumar, M.T. Jeena, K. Kim, J.H. Ryu, Cancer-mitochondria-targeted photodynamic therapy with supramolecular assembly of HA and a water soluble NIR cyanine dye, Chem Sci, 12, 2017, 8351-8356.
[68] E. Gottlieb, S.M. Armour, M.H. Harris, C.B. Thompson, Mitochondrial membrane potential regulates matrix configuration and cytochrome c release during apoptosis, Cell Death Differ, 10, 2003, 709–717.
[69] J.D. Ly, D.R. Grubb, A. Lawen, The mitochondrial membrane potential (Δψm) in apoptosis; an update, Apoptosis, 8, 2003, 115–128.
[70] Y. Rai, R. Pathak, N. Kumari, D.K. Sah, S. Pandey, N. Kalra, R. Soni, B.S. Dwarakanath, A.N. Bhatt, Mitochondrial biogenesis and metabolic hyperactivation limits the application of MTT assay in the estimation of radiation induced growth inhibition, Sci Rep, 8, 2018, 1531.

SUPLEMENTARY INFORMATION

1. Materials

All reactions were carried under a dry nitrogen atmosphere using Standard Schlenk techniques. All chemicals, solvents, and reagents were of reagent grade quality and were used as purchased from commercial sources. All solvents were dried and purified as described by reported procedure [1]. 4-Nitrophthalonitrile [2] were prepared according to the literature procedure. 4-nitrophenol, were purchased from Sigma-Aldrich and used without further purification and chemical treatment.

2. 1.2. Equipment

The IR spectra were recorded on a Perkin Elmer 1600 FT-IR spectrophotometer using KBr pellets. ^{1}H-NMR and ^{13}C-NMR spectra were recorded on a Varian Mercury 400 MHz spectrometer in $CDCl_3$. Chemical shifts were reported (δ) relative to Me_4Si as internal standard. MALDI-MS of complexes were obtained in dihydroxybenzoic acid as MALDI matrix using nitrogen laser accumulating 50 laser shots using Bruker Microflex LT MALDI-TOF mass spectrometer and Micromass Quatro LC/ULTIMA LC-MS/MS spectrometer. Elemental analysis equipment is EUROVECTOR EURO EA3000. Optical spectra in the UV-vis region were recorded with a Perkin Elmer Lambda 25 spectrophotometer.

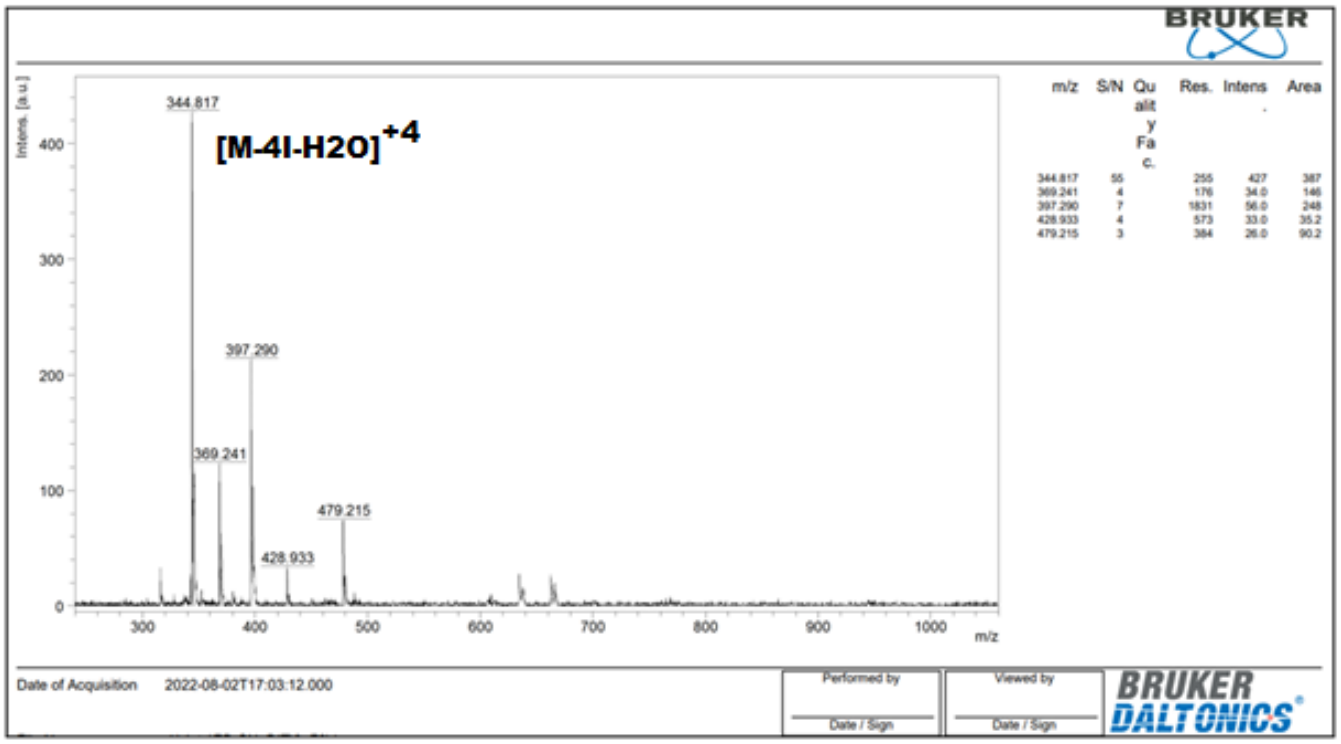

S. Figure 1. MALDI-TOF specta of 2(3), 9(10), 16(17), 23(24)-tetrakis-[N-methyl-(1-benzylpiperidin-4-yl)oxy)phthalocyaninato]zinc(II) iodide.

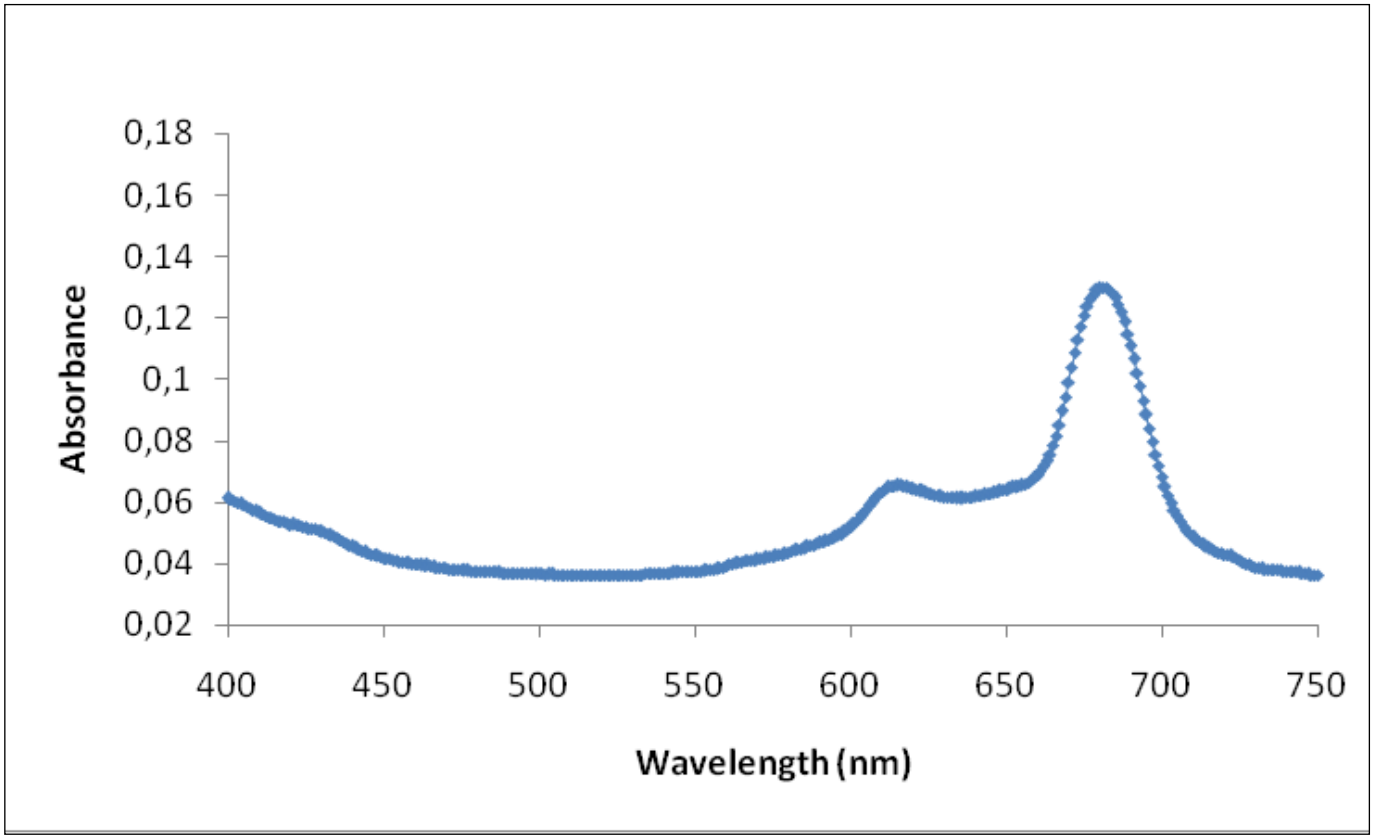

S. Figure 2. UV-Vis spectrum of 2(3), 9(10), 16(17), 23(24)-tetrakis-[N-methyl-(1-benzylpiperidin-4-yl)oxy)phthalocyaninato]zinc(II) iodide in water.

AR42J
(Figure 7A statistics)

24 h incubation
Dose comparisons

Post Hoc Tests

dose

Multiple Comparisons

Dependent Variable: perc
LSD

(I) dose	(J) dose	Mean Difference (I-J)	Sig.	95% Confidence Interval	
				Lower Bound	Upper Bound
,00	1,50	14,1738	,585	-45,9040	74,2516
	3,00	34,6694	,208	-25,4084	94,7472
	6,00	13,5145	,602	-46,5633	73,5923
	12,00	29,3381	,277	-30,7397	89,4158
1,50	,00	-14,1738	,585	-74,2516	45,9040
	3,00	20,4956	,475	-45,3163	86,3075
	6,00	-,6593	,981	-66,4712	65,1526
	12,00	15,1643	,593	-50,6476	80,9762
3,00	,00	-34,6694	,208	-94,7472	25,4084
	1,50	-20,4956	,475	-86,3075	45,3163
	6,00	-21,1549	,461	-86,9668	44,6570
	12,00	-5,3313	,849	-71,1432	60,4806
6,00	,00	-13,5145	,602	-73,5923	46,5633
	1,50	,6593	,981	-65,1526	66,4712
	3,00	21,1549	,461	-44,6570	86,9668
	12,00	15,8236	,578	-49,9883	81,6355
12,00	,00	-29,3381	,277	-89,4158	30,7397
	1,50	-15,1643	,593	-80,9762	50,6476
	3,00	5,3313	,849	-60,4806	71,1432
	6,00	-15,8236	,578	-81,6355	49,9883

Based on observed means.
The error term is Mean Square(Error) = 723,390.

48 h incubation
Dose comparisons

Post Hoc Tests

dose

Multiple Comparisons

Dependent Variable: perc
LSD

(I) dose	(J) dose	Mean Difference (I-J)	Sig.	95% Confidence Interval	
				Lower Bound	Upper Bound
,00	1,50	-7,4313	,161	-18,4332	3,5706
	3,00	1,4629	,770	-9,5390	12,4648
	6,00	14,1327*	,017	3,1308	25,1345
	12,00	32,6810*	,000	21,6791	43,6829
1,50	,00	7,4313	,161	-3,5706	18,4332
	3,00	8,8942	,071	-,9462	18,7346
	6,00	21,5639*	,001	11,7236	31,4043
	12,00	40,1123*	,000	30,2719	49,9527
3,00	,00	-1,4629	,770	-12,4648	9,5390
	1,50	-8,8942	,071	-18,7346	,9462
	6,00	12,6698*	,017	2,8294	22,5101
	12,00	31,2181*	,000	21,3777	41,0585
6,00	,00	-14,1327*	,017	-25,1345	-3,1308
	1,50	-21,5639*	,001	-31,4043	-11,7236
	3,00	-12,6698*	,017	-22,5101	-2,8294
	12,00	18,5483*	,002	8,7080	28,3887
12,00	,00	-32,6810*	,000	-43,6829	-21,6791
	1,50	-40,1123*	,000	-49,9527	-30,2719
	3,00	-31,2181*	,000	-41,0585	-21,3777
	6,00	-18,5483*	,002	-28,3887	-8,7080

Based on observed means.
The error term is Mean Square(Error) = 28,384.

S. Figure 3. Detailed statistical analyses for cytotoxicity

AR42J
(Figure 8A statistics)

24 h incubation
Dose comparisons

Post Hoc Tests

Dose

Multiple Comparisons

Dependent Variable: MMP

LSD

(I) Dose	(J) Dose	Mean Difference (I-J)	Sig.	95% Confidence Interval	
				Lower Bound	Upper Bound
,00	1,50	73,0364	,792	-487,9434	634,0163
	3,00	165,3276	,552	-395,6523	726,3074
	6,00	63,5499	,819	-497,4300	624,5297
	12,00	66,9000	,809	-494,0799	627,8799
1,50	,00	-73,0364	,792	-634,0163	487,9434
	3,00	92,2911	,739	-468,6887	653,2710
	6,00	-9,4866	,973	-570,4664	551,4933
	12,00	-6,1364	,982	-567,1163	554,8434
3,00	,00	-165,3276	,552	-726,3074	395,6523
	1,50	-92,2911	,739	-653,2710	468,6887
	6,00	-101,7777	,714	-662,7576	459,2022
	12,00	-98,4276	,723	-659,4074	462,5523
6,00	,00	-63,5499	,819	-624,5297	497,4300
	1,50	9,4866	,973	-551,4933	570,4664
	3,00	101,7777	,714	-459,2022	662,7576
	12,00	3,3501	,990	-557,6297	564,3300
12,00	,00	-66,9000	,809	-627,8799	494,0799
	1,50	6,1364	,982	-554,8434	567,1163
	3,00	98,4276	,723	-462,5523	659,4074
	6,00	-3,3501	,990	-564,3300	557,6297

Based on observed means.
The error term is Mean Square(Error) = 264079,832.

48 h incubation
Dose comparisons

Post Hoc Tests

Dose

Multiple Comparisons

Dependent Variable: MMP

LSD

(I) Dose	(J) Dose	Mean Difference (I-J)	Sig.	95% Confidence Interval	
				Lower Bound	Upper Bound
,00	1,50	-15,5889	,967	-776,7808	745,6031
	3,00	10,3054	,978	-750,8865	771,4973
	6,00	-75,4469	,841	-836,6388	685,7451
	12,00	-120,3156	,749	-881,5075	640,8763
1,50	,00	15,5889	,967	-745,6031	776,7808
	3,00	25,8943	,945	-735,2976	787,0862
	6,00	-59,8580	,873	-821,0499	701,3339
	12,00	-104,7267	,781	-865,9186	656,4652
3,00	,00	-10,3054	,978	-771,4973	750,8865
	1,50	-25,8943	,945	-787,0862	735,2976
	6,00	-85,7523	,820	-846,9442	675,4396
	12,00	-130,6210	,728	-891,8129	630,5709
6,00	,00	75,4469	,841	-685,7451	836,6388
	1,50	59,8580	,873	-701,3339	821,0499
	3,00	85,7523	,820	-675,4396	846,9442
	12,00	-44,8687	,905	-806,0606	716,3232
12,00	,00	120,3156	,749	-640,8763	881,5075
	1,50	104,7267	,781	-656,4652	865,9186
	3,00	130,6210	,728	-630,5709	891,8129
	6,00	44,8687	,905	-716,3232	806,0606

Based on observed means.
The error term is Mean Square(Error) = 486215,751.

S. Figure 4. Detailed statistical analyses for mitochondrial membrane potential

References

[1] D.D. Perrin, W.L.F. Armarego, Purification of Laboratory Chemicals (2nd edn), Pergamon Press: Oxford, (1989).
[2] Y.G. Young, W. Onyebuagu, J Organomet Chem 55 (1990) 2155-2159.